A High Efficiency, Low Resistance Antibacterial Filter Formed by Dopamine-Mediated In Situ Deposition of Silver onto Glass Fibers

Journal Article

Author(s):
Sun, Zhaoxia; Kong, Ying; Lan, Liang; Meng, Yingchao (ID); You, Tianle; Pauer, Robin; Wang, Hao; Zhang, Yizhou; Tang, Min; deMello, Andrew; Liang, Yun; Hu, Jian; Wang, Jing (ID)

A High Efficiency, Low Resistance Antibacterial Filter Formed by Dopamine-Mediated In Situ Deposition of Silver onto Glass Fibers

Zhaoxia Sun, Ying Kong, Liang Lan, Yingchao Meng, Tianle You, Robin Pauer, Hao Wang, Yizhou Zhang, Min Tang,* Andrew deMello, Yun Liang, Jian Hu, and Jing Wang*

The coating of filter media with silver is typically achieved by chemical deposition and aerosol processes. Whilst useful, such approaches struggle to provide uniform coating and are prone to blockage. To address these issues, an in situ method for coating glass fibers is presented via the dopamine-mediated electroless metallization method, yielding filters with low air resistance and excellent antibacterial performance. It is found that the filtration efficiency of the filters is between 94 and 97% and much higher than that of silver-coated filters produced using conventional dipping methods (85%). Additionally, measured pressure drops ranged between 100 and 150 Pa, which are lower than those associated with dipped filters (171.1 Pa). Survival rates of Escherichia coli and Bacillus subtilis bacteria exposed to the filters decreased to 0 and 15.7%$\pm$1.49, respectively after 2 h, with no bacteria surviving after 6 h. In contrast, survival rates of *E. coli* and *B. subtilis* bacteria on the uncoated filters are 92.5% and 89.5% after 6 h. Taken together, these results confirm that the in situ deposition of silver onto fiber surfaces effectively reduces pore clogging, yielding low air resistance filters that can be applied for microbial filtration and inhibition in a range of environments.

1. Introduction

Indoor air quality has become an increasingly important issue since humans spend now between 80% and 90% of their time on indoor activities.[1] Airborne bioaerosols, including bacteria, fungi, and viruses pose threats to human health through both respiratory and heart diseases. Only a few pathogens on small particles (with diameters less than 2.5 µm) often cause infection.[2,3] Accordingly, the efficient removal of small particles has become a key element in indoor air ventilation systems and air purifiers. The term "high efficiency" when applied to air filtration describes filters capable of removing 0.3 µm dioctylphthalate (DOP) particles with an efficiency of at least 99.97%.[4] That said, it should also be noted that the proliferation of bioaerosols captured on the filter surface may also be a health hazard, they can be re-released into the indoor air via re-entrainment.[5–7] Consequently, there is a recognized need for highly efficient filters with antibacterial functionality.[8–11]

Filter media can be modified by antibacterial materials, including silver, zinc oxide, TiO_2, quaternary ammonium salts, and biomass materials (such as tannic acid and chitosan).[12–19] For example, a ZnO nanorod/PTFE membrane, fabricated by atomic layer deposition, was shown to yield filtration efficiencies of 99.99%, but at the expense of unacceptably high air

Z. Sun, L. Lan, T. You, M. Tang, Y. Liang, J. Hu
School of Light Industry and Engineering
South China University of Technology
Guangzhou 510640, China
E-mail: tangmin88@scut.edu.cn
Z. Sun, Y. Kong, J. Wang
Institute of Environmental Engineering
ETH Zürich
Zürich 8093, Switzerland
E-mail: jing.wang@ifu.baug.ethz.ch

Z. Sun, Y. Kong, R. Pauer, J. Wang
Laboratory for Advanced Analytical Technologies
Empa
Swiss Federal Laboratories for Materials Science and Technology
Dübendorf 8600, Switzerland
Y. Meng, A. deMello
Department of Chemistry & Applied Biosciences
ETH Zürich
Zürich 8093, Switzerland
H. Wang
National Key Laboratory of Nuclear, Biological and Chemical Disaster Protection
Academy of Chemical Prevention
Academy of Military Sciences
Beijing 100191, China
Y. Zhang
School of Environmental and Chemical Engineering
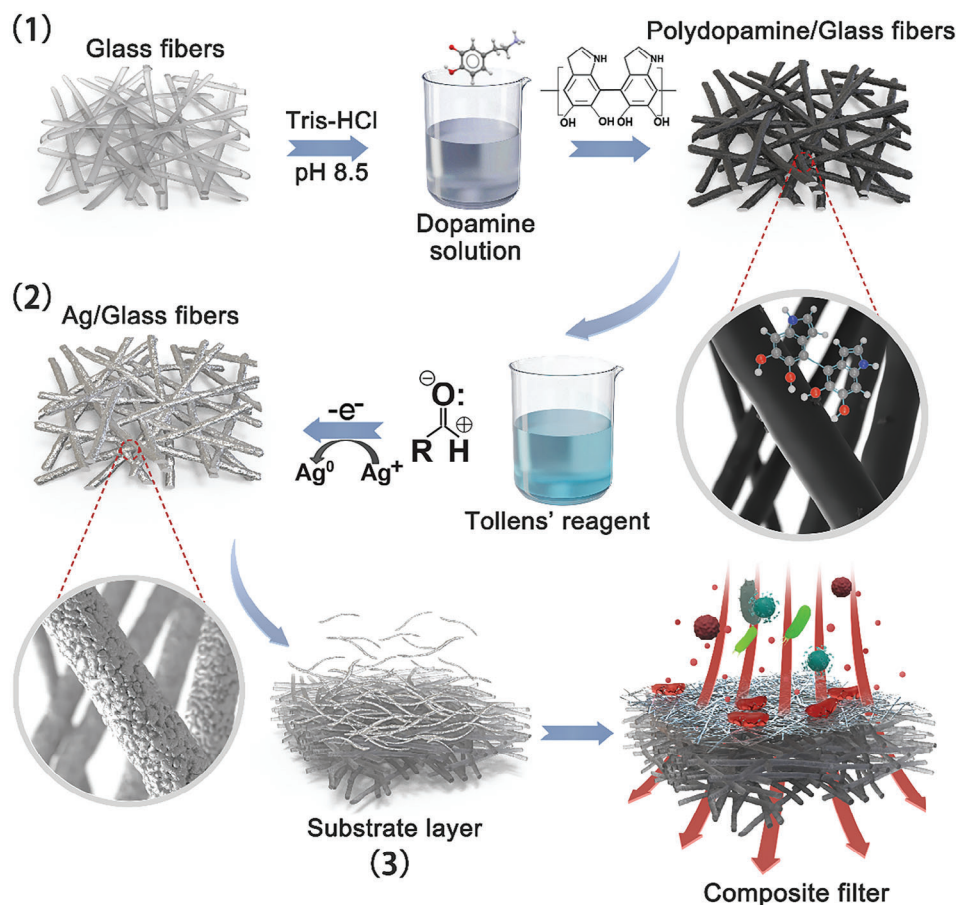Shanghai University
Shanghai 200444, China

Figure 1. Schematic of the workflow used to fabricate Ag/glass fiber composite filter media. a) Fibers are coated with polydopamine, forming annular films along the fibers' axial direction. b) Silver forms on the surface of the fibers, with polydopamine serving as the primer. c) Silver-coated fibers are deposited on the substrate layer by the wet-laid method, forming composite air filter media fibers with antimicrobial properties.

resistance (900 Pa @ 11 cm s^{-1}).[12] Aerosol processes can also be used to deposit antibacterial agents onto filter media in a direct manner. For example, Jung et al. fabricated antibacterial filters by continuously depositing Ag/carbon nanotube particles onto an air filter medium through aerosol loading.[20] These filters exhibit excellent antibacterial performance, with microbial viability on the filters being reduced to 10% after 100 min. Unfortunately, the air resistance associated with these filters is non-ideal due to pore blockage, leading to high energy consumption during operation. Finally, it should be noted that antibacterial agents can also be added via electrospinning, with electrospun nanofibers embedded with silver or silver nanoparticles being used as filter media.[21,22] However, they can't be used for highly efficient filters due to their poor and unreliable mechanical strength.

Dopamine-mediated coating method has been reported to be versatile for a wide range of substrates due to its simple ingredients, mild reaction condition, and applicability to multiple types of materials with complex shapes.[23–27] Polydopamine initially forms a thin film on the surface of the substrate and then the catechols in polydopamine with metal-binding ability serve as primers for the reduction of metal ions. In situ metal will form on the substrate surface. This simple metallization process provides a convenient and effective approach to the prepa-

ration of metalized materials. Xu et al.[28] coated the cotton fabric with a thin adherent polydopamine membrane and Ag$^+$ was in situ reduced on the polydopamine to Ag^0 nanoparticles. which showed durable antibacterial activity. Zhang et al.[29] coated PDA on graphene oxide (GO) by polymerizing dopamine (DA) at room temperature. During the process, GO was reduced by the DA. The PDA layer on the surface of graphene nanosheets (GNS) can be used as a nanoscale guide to form uniform AgNPs on the surface of PDA-GNS. The Ag-PDA-GNS hybrid materials exhibited strong antibacterial properties. Xie et al.[30] grafted the nano-Ag on the bacterial cellulose (BC) by dopamine illustrating that the BC antimicrobial composites by PDA in situ reduction of nano-Ag had a great potential as an antibacterial dressing. Generally, the relevant works show the effective dopamine-mediated method to coat silver nanoparticles on the substrate material. In this work, we employed this in situ deposition method to avoid pore blockage during the fabrication process which is crucial for the porous air filter media energy consumption. In this study, we present the antibacterial silver-coated filter media possessing high filtration efficiencies and low associated pressure drops. To generate uniform coatings and reduce pore blockage the dopamine-mediated in situ deposition method is applied.

**ADVANCED
SCIENCE NEWS**

www.advancedsciencenews.com

NANO · MICRO

small

www.small-journal.com

Table 1. Brief description of the abbreviations of the different filter media.

Abbreviations of filter media	Description
P-Control	Consists of pristine glass fibers
P-0.5	Consists of silver-coated glass fibers (F-0.5) with a fiber concentration of 0.5 g L^{-1} in the reaction solution
P-1.0	Consists of silver-coated glass fibers (F-1.0) with a fiber concentration of 1.0 g L^{-1} in the reaction solution
P-1.5	Consists of silver-coated glass fibers (F-1.5) with a fiber concentration of 1.5 g L^{-1} in the reaction solution
P-Dipped	Glass fiber filter media coated by silver by dipping method

These filter media consist of conformal silver-coated glass wool fibers produced by dopamine-mediated electroless metallization. **Figure 1** schematically illustrates the fabrication of Ag/glass fiber composite filter media. First, the glass wool fibers are coated with polydopamine with different concentrations in the solution. Second, the polydopamine-coated fibers are coated with silver by Tollens' reagent. Last, the silver-coated fibers are applied to fabricate filter media by the wet-laid method.

2. Results and Discussion

2.1. Morphology and Diameter of Silver-Coated Fibers

The composite filter media fabricated in this work consists of two layers. The substrate layers are formed by glass fibers with a diameter of 6–8 μm and the top layers are formed by the glass wool fibers. A brief description of the abbreviations of the different filter media is shown in **Table 1**. **Figures 2a,b** present scanning electron microscopy (SEM) images of the surface of P-control (filter media consisting of pristine glass fibers) and P-dipped (filter media coated with silver by dipping method). It can be seen that some silver agglomerates form and block pores in the fiber network. Conversely, there is no pore-clogging in the filter media coated using the polydopamine-mediated method (Figure 2c) due to the fact that annular silver layers are formed along the axial fiber direction). During the coating process, polydopamine initially forms a thin film on the surface of the fiber and then serves as a primer for silver reduction.[23,26,27] In situ silver formation leads to an annular layer along the axial direction of the fiber. A 254±40 nm thick silver layer forms on the surface of a glass fiber when using a fiber concentration of 0.5 g L^{-1} in the reaction solution. The silver layers become thinner as the fiber concentration in the reaction solution increases. Some defects in the silver layer (along the axial direction) are observed (Figure S1, Supporting Information). The silver content of the P-0.5, P-1.0, and P-1.5 filters are 29.9%, 14.1%, and 6.5%, respectively (Table S2, Supporting Information). Although P-1.5 and P-Dipped have similar basic weights and silver contents, there are fewer silver agglomerates in P-1.5.

Figure 2d shows elemental mapping by energy-dispersive X-ray spectroscopy (EDS) of a cross-section of silver-coated glass fibers (F-0.5). Here, the silver signal matches the nanofiber to-

pography, confirming that the glass fibers have been successfully coated with silver.

Figure 2e shows the diameter distribution of glass wool fibers before and after silver coating, with the fiber concentration in the reaction solution being 0.5 g L^{-1} (F-0.5), 1.0 g L^{-1} (F-1.0), and 1.5 g L^{-1} (F-1.5). The diameters of the pristine glass fibers typically range from 60 to 365 nm with an average diameter of 362 nm. The silver coating leads to an increase in the total fiber diameter. The average diameter of the F-0.5 is 867 nm and those of the F-1.0 and F-1.5 are 710 and 693 nm, respectively.

Figure 2f shows the X-ray diffraction (XRD) patterns of the fibers before and after silver deposition. The peaks at 38.3°, 44.6°, 64.7°, 77.6°, and 81.8° are assigned to the diffraction from the (111) (200) (220) (331), and (222) planes of the face-centered cubic structure of silver, respectively.[31]

2.2. Properties of Filter Media

The initial filtration efficiency of P-control against NaCl particles (with a mean mass diameter of 260 nm) is 99.69%. After being coated with silver via dipping, the filtration efficiency decreases to 85.1%, and the pressure drop increases to 171.1 Pa (**Figure 3a,b**). The filtration efficiencies and pressure drop associated with the P-0.5, P-1.0, and P-1.5 filters are 94.03%, 94.74%, 96.95%, and 107.8, 123.8, and 149.9 Pa, respectively. According to single-fiber filtration theory, filtration efficiency is inversely proportional to fiber diameter and the porosity of the filter medium.[32] The initial filtration efficiency of the filter media consisting of silver-coated fibers is lower than that of the pristine glass fibers filter media. This is due to the increase in fiber diameter and porosity of filter media, which also indicates increased air permeability (Table S2, Supporting Information). Moreover, the initial filtration efficiency of the filter medium increases as the diameter of silver-coated fibers decreases. The quality factor (QF) of the P-1.5 sample is the smallest (0.024 Pa^{-1}) due to the largest pressure drop (Figure 3c). For the four types of silver-coated filter medium, the lowest filtration efficiency and highest pressure drop are associated with the P-Dipped sample and a QF of 0.014 Pa^{-1}.

Figure 3d shows velocity field simulations for each filter medium. The differences in velocity in the ultrafine fiber layers are attributed to their different porosity values, which are related to their mass and thickness. Figure 3e shows the pressure drop across the filter media at different face velocities of 0.03, 0.05, 0.1, and 0.15 m s^{-1}. The linear relationship between pressure drop and face velocity is in accordance with Darcy's law.[32] The pressure drop for P-0.5 is the smallest of the three types of silver-coated fibers for a given face velocity. Here, the large fiber diameter contributes to the large thickness and porosity of the filter medium, as shown in Figure S2 (Supporting Information). This in turn ensures reduced air resistance. Figure 3f presents the variation of filtration efficiency with NaCl particle diameter for the different filter media at the face velocity of 0.05 m s^{-1}. All curves exhibit a "U-shaped" form, with the most penetrating particle size being ≈200 nm. The filtration efficiency of P-0.5 is the lowest due to their largest fiber diameter and smallest specific surface area. Additionally, the filtration efficiency of P-1.5 is close to that of the control sample. As shown in Figure 3b, the pressure drop for P-1.5 is lower than that of P-control (which consists of

**ADVANCED
SCIENCE NEWS**

www.advancedsciencenews.com
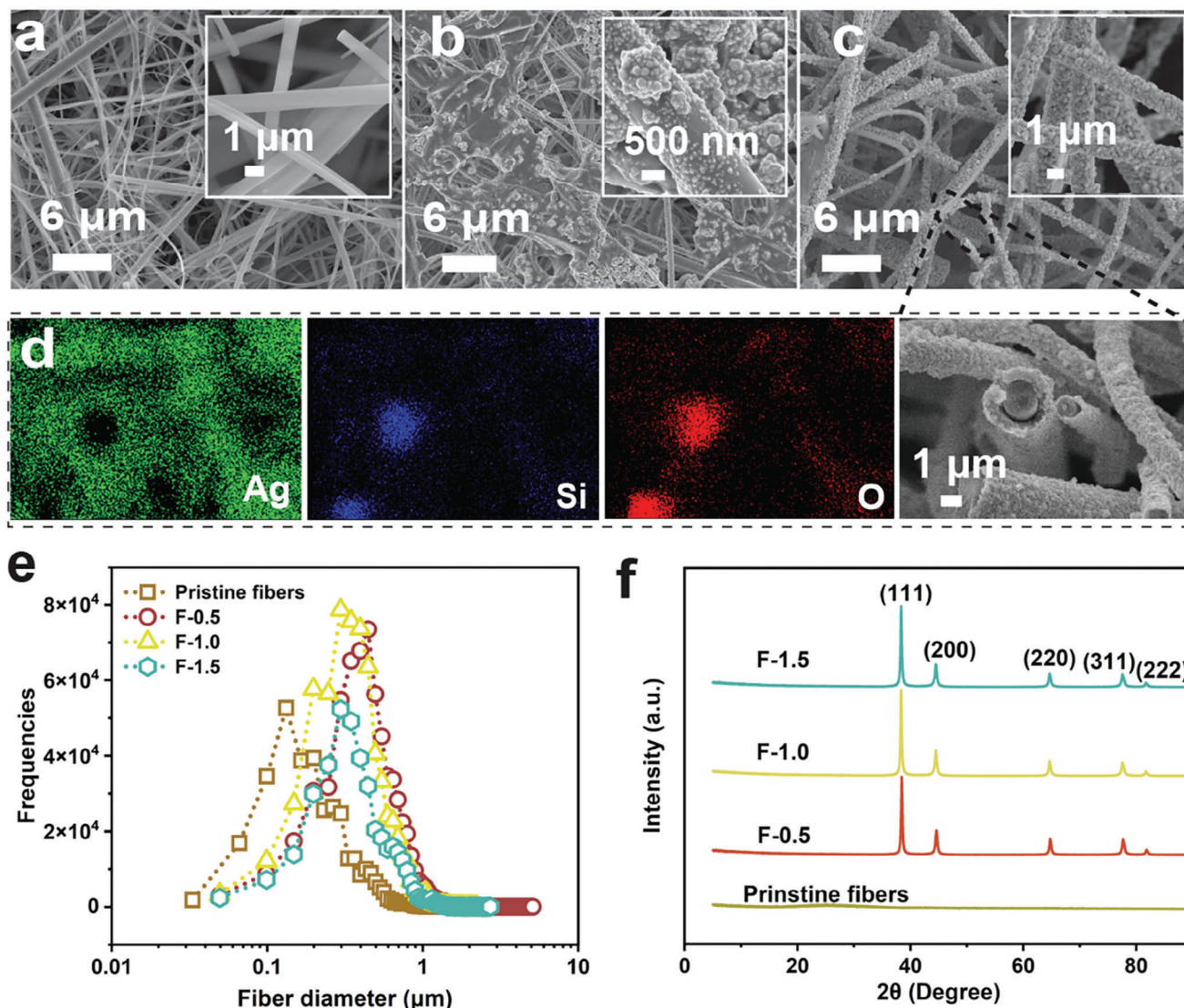
NANO · MICRO

small

www.small-journal.com

Figure 2. SEM image of filter media a) P-control, b) P-dipped, c) P-0.5 and d) SEM image of silver-coated glass fibers (F-0.5), with elemental mapping of Si, O, and Ag via energy-dispersive X-ray spectroscopy, e) Fiber diameter distribution for pristine glass fibers, F-0.5, F-1.0, and F-1.5, f) XRD patterns of pristine and silver coated glass fibers.

pristine fibers). This indicates that the deposition of silver on the fiber surface leads to high filtration efficiencies and low-pressure drop.

2.3. Antibacterial Performance

Figure 4 reports the antibacterial performance of the filter media against gram-negative (*E. coli*) and gram-positive (*B. subtilis*) bacteria according to the method described in Figure 4a. The sterilized filter media was dipped with the bacteria solution and washed with the sterilized water from the filter media after different contact time. The elution is spread on agar plates and fluorescence imaging to evaluate the survival rate of bacteria. Figure 4b shows that the survival rates of *E. coli* bacteria (OD$_{600}$ value, the optical density of bacteria suspension mea-

sured by a UV spectroscopy at a wavelength of 600 nm, is 0.15) exposed to P-control, P-0.5, P-1.0, and P-1.5 for 2 h decreases to 98.2%, 3.6%, 0.01%, 0.003%, respectively. Furthermore, no colony-forming units (CFUs) can be observed after the *E. coli* bacteria are exposed to the filter media P-1.0 and P-1.5 (Figure S4a, Supporting Information) for a period of 4 h.

The survival rates of *B. subtilis* bacteria (OD$_{600}$ value is 0.5) exposed to P-control, P-0.5, P-1.0, and P-1.5 filter media for 2 h decreases to 95.1%, 28.9%, 21.0%, and 15.7%, respectively (Figure 4c). However, the survival rate of *B. subtilis* bacteria (OD$_{600}$ value is 0.2) on P-0.5, P-1.0, and P-1.5 filter media decreases to 10%, 0.4%, and 0% respectively after 2 h. The survival rate of *E.coli* and *B. subtilis* bacteria with average initial concentrations of 1.03×10^5 cells mL^{-1} and 7.56×10^5 cells mL^{-1} exposed to the P-control filter media for 6 h remains at 92.5% and 82.0%, respectively. The sharply decreased

ADVANCED
SCIENCE NEWS
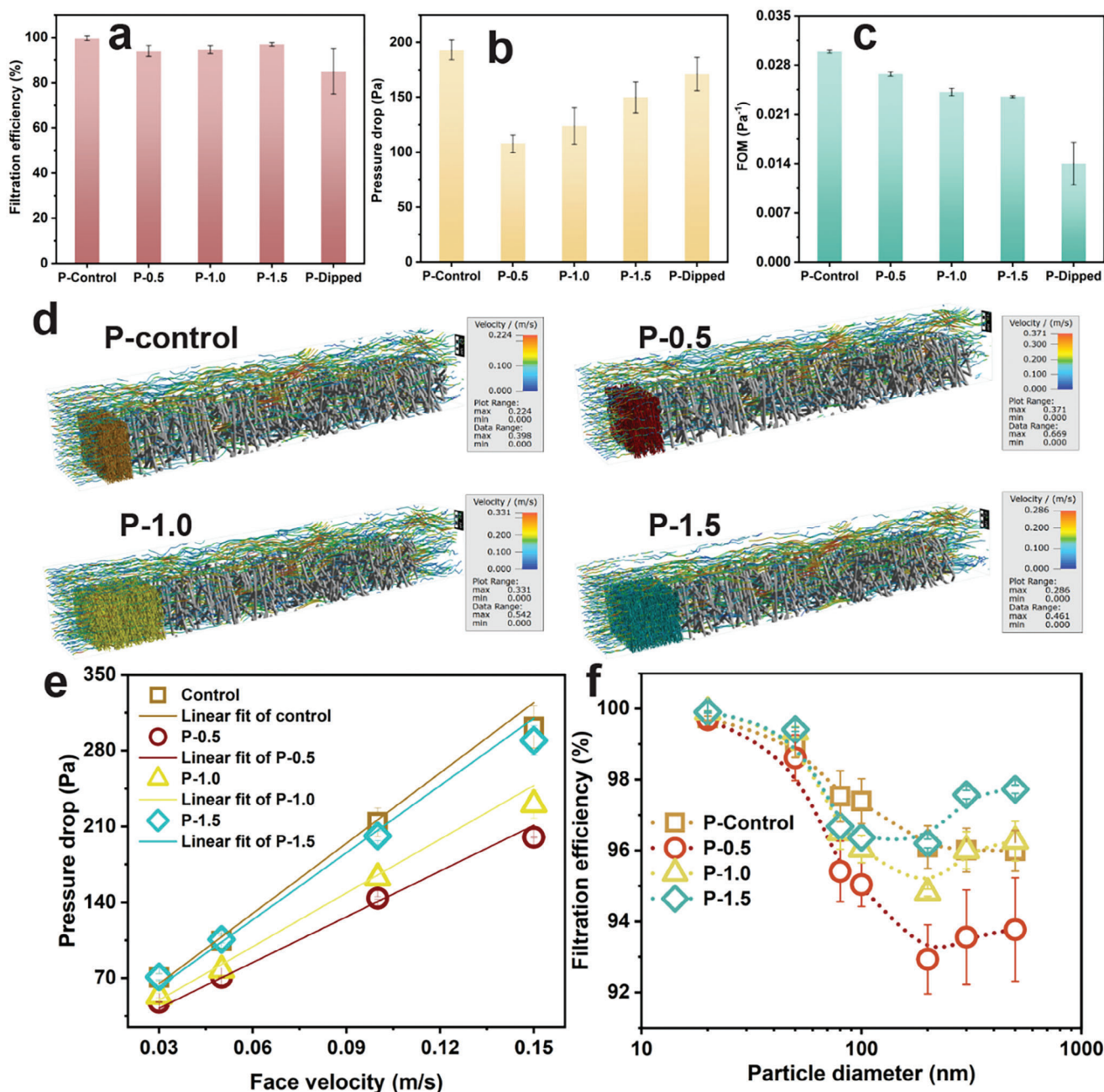www.advancedsciencenews.com

NANO · MICRO
small
www.small-journal.com

Figure 3. a) Initial filtration efficiency, b) Pressure drop, and c) Figures of merit for each filter medium against NaCl particles (0.26 μm, @5.3 cm s^{-1}). d) Simulation of velocity distribution in P-control, P-0.5, P-1.0, and P-1.5. e) Pressure drop of these four kinds of filter media at different face velocities of 0.03, 0.05, 0.1, and 0.15 m s^{-1}. f) Filtration efficiency of these four kinds of filter media against NaCl particles with different mobility diameters at the face velocity of 0.05 m s^{-1}.

survival rate of these two kinds of bacteria on the P-0.5, P-1.0, and P-1.5 filter media after only 2 h of contact indicates that the silver-coated fibers can inactivate bacteria rapidly and effectively. The survival rate of bacteria loaded on filter media P-1.5 is the smallest contributing to their smallest average fiber diameter (Table S2, Supporting Information) and the largest specific surface area. This increase in surface area provides for more contact sites with bacteria and releases silver ions more efficiently.

Fluorescence images of bacteria eluted from the filter media after different contact durations indicate a clear change in the proportion of live and dead *E.coli* and *B. subtilis* bacteria (Figure 4d). Conversely, morphological variations in the bacteria are not evident after contact with control filter media for 6 h in the condition of 97% relative humidity (RH, Figure S5b, Supporting Information). Figure 4e shows the morphology of bacteria exposed to the P-1.5 filter, with bacteria flattening and aggregating after contact with the silver-
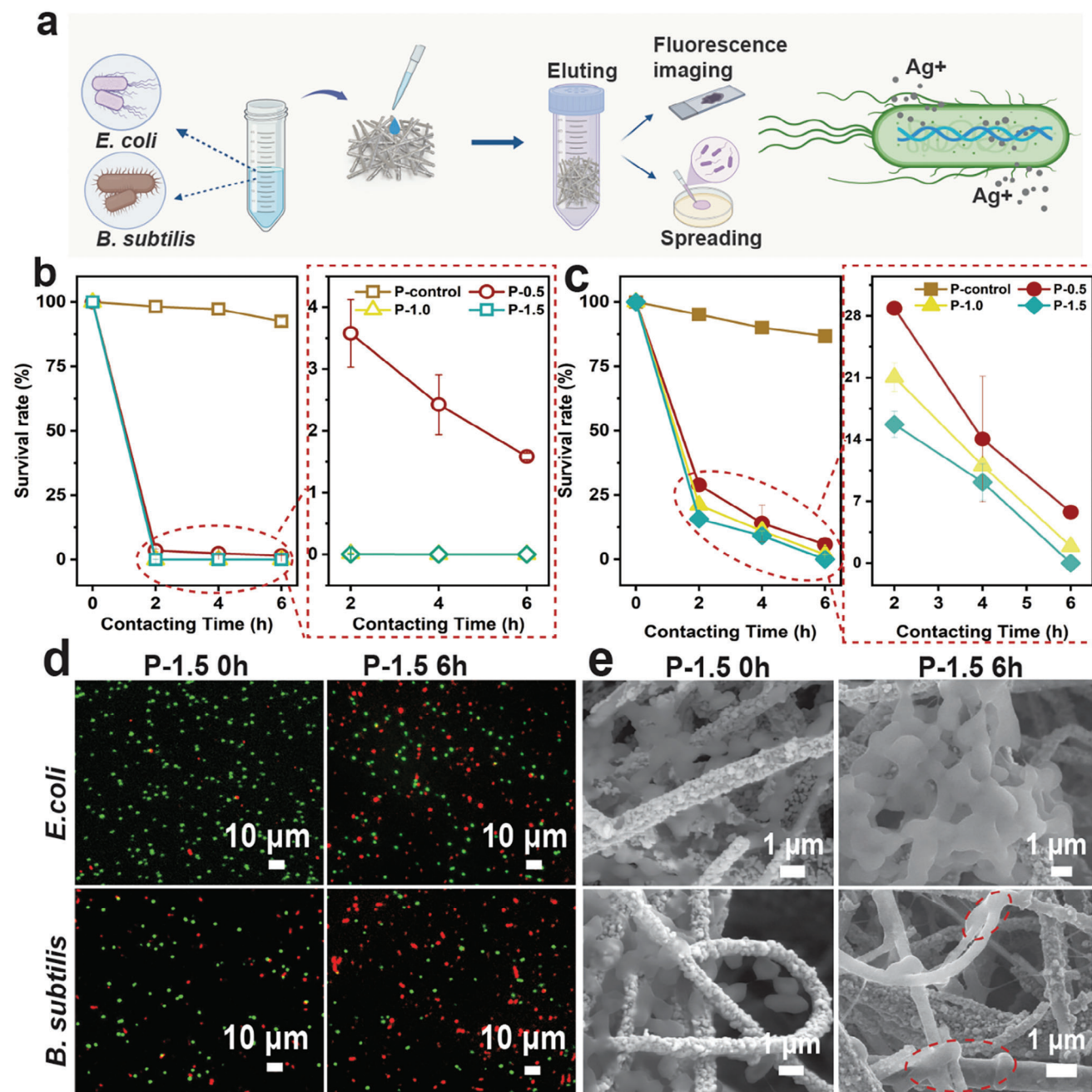
Figure 4. Antibacterial properties of the developed filters. a) The experimental workflow and schematic of the proposed antibacterial mechanism of the filter media. b) The survival rate of *E. coli* bacteria contacting silver-coated glass fiber filter media as a function of time. c) The survival rate of *B. subtilis* bacteria contacting silver-coated glass fiber filter media as a function of time. d) Fluorescence images and e) SEM images of *E. coli* and *B. subtilis* bacterial exposed to P-1.5 for different durations.

coated filter medium for 6 h. Significantly, silver cations released from the fibers interact with proteins and other components in the bacterial membrane, leading to the inactivation of proteins and structural changes in the cell wall and nuclear membrane. As a result, DNA molecules condense and lose their ability to replicate as silver ions penetrate. Thiol (-SH) groups in proteins are also inactivated through interaction with silver ions.[33–35] As can be seen in

Figure 4e, some bacteria cells also collapse (indicated by the red dotted line) due to their inability to maintain osmotic pressure.

Ensuring high filtration efficiency, low-pressure drops, and effective antibacterial efficiency is key to the development of the air filter media described herein. In addition to the antibacterial efficiency, the figure of merit for the P-1.5 filter medium is 0.023 Pa^{-1}. This value is highly competitive when compared to

previously reported materials (Table S1, Supporting Information).

3. Conclusion

The antibacterial performance of high-efficiency filters in indoor air cleaning systems has attracted widespread attention, due to a growing awareness of pathogens spurred by the COVID-19 pandemic. In this study, we have fabricated highly efficient filter media consisting of silver-coated glass fibers via dopamine-mediated in situ electroless deposition. Compared to silver-coated glass fibers fabricated by conventional dipping methods, media produced by our dopamine-mediated in situ deposition method have higher filtration efficiencies and significantly lower pressure drops (attributed to reduced pore blockage during coating).

Additionally, the silver-coated fiber media show excellent antibacterial performance, with the survival rate of *E.coli* and *B. subtilis* bacteria decreasing sharply after exposure to the filter media for 2 h. Silver cations released from the surface of the fibers interact with proteins and other components of the bacterial membrane, leading to the inactivation of proteins and structural changes in the cell wall and nuclear membrane. The high-efficiency filter media with antibacterial properties suggest immediate and outstanding potential for a range of air purification applications.

4. Experimental Section

Fabrication of Filter Media Consisting of Silver-Coated Glass Fibers: Glass fibers (0.0238 g) with diameters between 60 and 350 nm were dispersed in deionized water by high-speed vortex and then filtered by stainless steel wire mesh (with a pore diameter of 50 μm). Fibers were treated with a 2 g L^{-1} dopamine (DA)-HCl solution, which was prepared by dissolving DA-HCl powder in a 10 mM Tris-HCl solution with a pH of 8.5 for 12 h. Subsequently, fibers coated with polymerized DA were sonicated in deionized water for 5 min to remove non-uniformly aggregated polydopamine (PDA) particles and water was removed by filtering. The Ag precursor for electroless plating was prepared by drop-wise addition of the aqueous ammonia solution (28%–30%) to AgNO$_3$ (20 g L^{-1}) until the precipitated silver oxide was completely dissolved. Initially, hydroxide (OH$^-$) converts silver ions (Ag$^+$) into brown silver oxide. Silver oxide was then dissolved by adding a sufficient amount of aqueous ammonia, forming [Ag(NH$_3$)$_2$]$^+$. PDA-coated fibers were dispersed in the silver precursor solution and glucose was added to the reaction at a concentration of 40 g L^{-1} with continuous stirring. Fibers were filtered after 15 min and then ultrasonicated for 3 min and washed 3 times with deionized (DI) water to remove aggregated silver particles. Silver-coated fibers were dispersed in DI water and then deposited on the substrate layer by the wet-laid method. Subsequently, the wet filter media were dried in an oven at 50 °C for 8 h.

The glass filter media were also coated with silver by the dipping method for comparison with the filter media coated by in situ deposition method. In brief, the glass fibers were dispersed in DI water and then deposited on the substrate layer. The dry composite filter media were immersed in the Ag precursor solution (10 mL) which was mentioned before for 1 h in dark. Then the filter media were immersed in the glucose solution (40 g L^{-1}) for 1 h. The coated filter media were rinsed 3 times with distilled water. At last, they were dried in the oven at 50 °C for 8 h.

Characterization of Fibers: The surface morphology and corresponding EDS elemental mapping of the silver-coated fibers were visualized by a field emission scanning electron microscope (SU 5000, Hitachi, Japan). Fiber diameters were calculated using Image-J image analysis software. The X-ray diffraction patterns (XRD) of all samples were recorded

on a Bruker D8 Advance X-ray diffractometer with Cu K$_\alpha$ radiation ($\lambda = 1.5418$ Å). The powder was leveled on the sample holder and scanned with a 2θ angle from 5 to 90°, with a step speed of 2° min^{-1}.

Characterization of Filter Media: The morphology of the filter media was analyzed by field emission scanning electron microscope (SU 5000, Hitachi, Japan). The silver content was calculated as follows

$$C = \frac{m_s - m_c}{m_c} \times 100 \tag{1}$$

where m_s is the weight of the filter media consisting of silver-coated fibers, and m_c is the weight of the filter media consisting of pristine fibers. The initial filtration efficiency and pressure drop against NaCl particles (with a median diameter of 0.26 μm) were measured by an automated filter tester (model 8130, TSI, USA) at a face velocity of 5.3 cm s^{-1}. The figure of merit for filter media, which was used to evaluate the quality of filter media, was defined as follows

$$FOM = \frac{-\ln P}{\Delta p} \tag{2}$$

where P is the penetration rate of particles in the filter media and Δp is the pressure drop of filter media. The pressure drops at face velocities of 3, 5, 10, and 15 cm s^{-1} were measured. 3D digital models of the filter media were reconstructed using Geodict software (Math2Market, Germany) based on the fiber diameters, thickness, and air permeability of filter media. The velocity fields in four kinds of filters were simulated using a velocity of 5.3 cm s^{-1}.

The filtration efficiency of the filters against the sodium chloride particles, with mobility diameters of 20, 50, 80, 100, 200, 300, and 500 nm, was measured. A schematic diagram of the experimental setup is shown in Figure S3 (Supporting Information). Monodisperse NaCl particles with mobility diameters of 20, 50, and 80 were selected by a differential mobility analyzer (DMA, model 3081, TSI, USA) from polydisperse particles generated by the NaCl solution at 0.01 wt% using an atomizer (model 3079A, TSI, USA). The particles with mobility diameters of 100, 200, 300, and 500 nm were selected from the polydisperse particles generated by a NaCl solution at 1.0 wt%. Particles generated from the atomizer (before passing through the DMA) were dried using a diffusion dryer. A soft X-ray neutralizer (model 3088, TSI, USA) was used to neutralize the selected particles from DMA to the Boltzmann charge distribution state. A condensation particle counter (CPC, 3776, TSI, USA) was used for particle concentration measurement upstream and downstream of the filter medium. The effective filtration area of the filters was 5.0 cm^2 and the face velocity was 5.0 cm s^{-1}. The flow rate of the test system was controlled by a mass flow controller. The filtration efficiency of filters was calculated according to,

$$E = 1 - \frac{C_{down}}{C_{up}} \tag{3}$$

where, C_{up} and C_{down} were the particle number concentrations in the upstream and downstream of the filters, respectively.

Antibacterial Performance of Filter Media: A schematic experimental setup to evaluate the antibacterial properties of the filter media is shown in Figure 4a. First, a round filter with a diameter of 39 mm was cut into four equal pieces. These pieces were then sterilized by UV light for 1 h. 50 μL bacteria suspension (*E. coli* bacteria suspension OD$_{600}$ = 0.15, ≈2.0 × 10^7 cell mL^{-1}, *B. subtilis* bacteria suspension OD$_{600}$ = 0.5, ≈3.0 × 10^7 cell mL^{-1}, OD$_{600}$ = 0.2, ≈1.2 × 10^6 cell mL^{-1}) was delivered onto the UV treated filter media pieces. The filter pieces (loaded with bacteria) were put into a homemade incubator with a relative humidity of between 92 and 95%. After 0, 2, 4, and 6 h, filter media pieces were put into centrifuge tubes with 5 mL of sterilized water, after being taken out from the incubator. Next, the tubes were vortexed for 15 min to extract bacteria from the filter media pieces into the water. Then, 100 μL of *E. coli* or *B. subtilis* suspension was spread onto LB agar plates. The agar plates were

cultured in an incubator at 37°C for 24 h to allow estimation of colony-forming units.

Bacteria were washed in sterilized water and stained with NucBeacon Green according to the suggestion of ViaQuant Viability/Cytotoxicity kit for bacteria cells (Cat. A180, GeneCopoeia, Inc.). The stained bacteria were imaged using fluorescence microscopy (Eclipse Ti-E inverted microscope, Nikon, Zurich, Switzerland). In the fluorescence images, green fluorescence indicates live bacteria. The morphology of *E. coli* bacteria and *B. subtilis* bacteria loaded onto different filter media was characterized using an environmental scanning electron microscope (ESEM, Quanta 650, FEI, USA).

Statistical Analysis: Statistical Analysis was conducted using Excel (Office 2019, Microsoft, USA), and Image J software. All data were presented as mean ± s.d. Five samples were tested for filtration efficiency and pressure drop analyze. For each of the antibacterial performance evaluation experiments described here, data were collected from three replicate tests. For each test the bacteria eluate was plated in triplicate resulting in a total of nine data points for each experiment.

Supporting Information

Supporting Information is available from the Wiley Online Library or from the author.

Conflict of Interest

The authors declare no conflict of interest.

Data Availability Statement

The data that support the findings of this study are available on request from the corresponding author. The data are not publicly available due to privacy or ethical restrictions.

Keywords

[1] N. E. Klepeis, W. C. Nelson, W. R. Ott, J. P. Robinson, A. M. Tsang, P. Switzer, J. V. Behar, S. C. Hern, W. H. Engelmann, *J Expo Sci Environ Epidemiol* **2001**, *11*, 231.

[2] S. Raju, T. Siddharthan, M. C. McCormack, *Clin Chest Med* **2020**, *41*, 825.

[3] J. Sun, J. Wang, J. Yang, X. Shi, S. J. Li, J. P. Cheng, S. Chen, K. Sun, Y. R. Wu, *BMC Public Health* **2022**, *22*, 767.

[4] EN 1822-1-2009 High efficiency air filters (EPA, HEPA, and ULPA) – Part 1: Classification, performance testing, marking **2009**.

[5] R. A. Stern, A. Al-Hemoud, B. Alahmad, P. Koutrakis, *Sci. Total Environ.* **2021**, *782*, 146799.

[6] Z. Sun, Y. Yue, W. He, F. Jiang, C. Lin, D. Y. Pui, Y. Liang, J. Wang, *Build. Environ.* **2020**, *180*, 107020.

[7] O. V. Pyankov, I. E. Agranovski, R. Huang, B. J. Mullins, *Clean: Air, Water* **2008**, *36*, 609.

[8] X. Zhang, Z. Ji, Y. Yue, H. Liu, J. Wang, *Environ. Sci. Technol.* **2020**, *55*, 4123.

[9] X. Zhang, J. Wang, *Clin. Infect. Dis.* **2021**, *73*, e241.

[10] M. Gao, X. Zhang, Y. Yue, T. Qiu, J. Wang, X. Wang, *J Hazard Mater.* **2022**, *430*, 128417.

[11] J. Malloy, A. Quintana, C. J. Jensen, K. Liu, *Nano Lett.* **2021**, *21*, 2968.

[12] Z. Zhong, Z. Xu, T. Sheng, J. Yao, W. Xing, Y. Wang, *ACS Appl. Mater. Interfaces* **2015**, *7*, 21538.

[13] B. Wang, Q. Wang, Y. Wang, J. Di, S. Miao, J. Yu, *ACS Appl Mater Interfaces* **2019**, *11*, 43409.

[14] S. Jeong, H. Cho, S. Han, P. Won, H. Lee, S. Hong, J. Yeo, J. Kwon, S. Ko, *Nano Lett.* **2017**, *17*, 4339.

[15] J. Choi, B. Yang, G. Bae, J. Jung, *ACS Appl Mater Interfaces* **2015**, *7*, 25313.

[16] Y. Wang, G. Xia, H. Yu, B. Qian, Y. Cheung, L. Wong, J. Xin, *Adv. Mater.* **2021**, *33*, 2100140.

[17] S. Shakya, Y. He, X. Ren, T. Guo, A. Maharjan, T. Luo, T. Wang, R. Dhakhwa, B. Regmi, H. Li, *Small* **2019**, *15*, 1901065.

[18] G. Applerot, J. Lellouche, A. Lipovsky, Y. Nitzan, R. Lubart, A. Gedanken, E. Banin, *Small* **2012**, *8*, 3326.

[19] K. C. Black, T. S. Sileika, J. Yi, R. Zhang, J. G. Rivera, P. B. J. Messersmith, *Small* **2014**, *10*, 169.

[20] J. Jung, G. Hwang, J. Lee, G. Bae, *Langmuir* **2011**, *27*, 10256.

[21] Y. Xiao, Y. Wang, W. Zhu, J. Yao, C. Sun, J. Militky, M. Venkataraman, G. Zhu, *Sep. Purif. Technol.* **2021**, *259*, 118135.

[22] A. Vanangamudi, S. Hamzah, G. Singh, *Chem. Eng. J.* **2015**, *260*, 801.

[23] H. Lee, S. M. Dellatore, W. M. Miller, P. B. Messersmith, *Science* **2007**, *318*, 426.

[24] H. Yang, Y. Lan, W. Zhu, W. Li, D. Xu, J. Cui, D. Shen, G. Li, *J. Mater. Chem.* **2012**, *22*, 16994.

[25] Y. Liao, Y. Wang, X. Feng, W. Wang, F. Xu, L. Zhang, *Mater. Chem. Phys.* **2010**, *121*, 534.

[26] J. H. Ryu, P. B. Messersmith, H. Lee, *ACS Appl Mater Interfaces* **2018**, *10*, 7523.

[27] T. S. Sileika, H. D. Kim, P. Maniak, P. B. Messersmith, *ACS Appl Mater Interfaces* **2011**, *3*, 4602.

[28] H. Xu, X. Shi, H. Ma, Y. Lv, L. Zhang, Z. Mao, *Appl. Surf. Sci.* **2011**, *257*, 6799.

[29] Z. Zhang, J. Zhang, B. Zhang, J. Tang, *Nanoscale* **2013**, *5*, 118.

[30] Y. Xie, L. Yue, Y. Zheng, L. Zhao, C. Liang, W. He, Z. Zhou, Y. Sun, Y. Yang, *Appl. Surf. Sci.* **2019**, *491*, 383.

[31] Y. Sun, Y. Xia, *Science* **2002**, *298*, 2176.

[32] J. Wang, S. Kim, D. Y. H. Pui, *J. Aerosol Sci.* **2008**, *39*, 323.

[33] A. Hamad, K. Khashan, A. Hadi, *J. Inorg. Organomet. Polym. Mater.* **2020**, *30*, 4811.

[34] W. Jung, H. Koo, K. Kim, S. Shin, S. Kim, Y. H. Park, *Appl. Environ. Microbiol.* **2008**, *74*, 2171.

[35] O. Golubeva, N. Ulyanova, E. Vladimirova, O. Shamova, *Langmuir* **2021**, *37*, 12356.